Supplement of Atmos. Chem. Phys., 24, 9059–9083, 2024
https://doi.org/10.5194/acp-24-9059-2024-supplement

Atmospheric Chemistry and Physics
Open Access
EGU

Supplement of

Differences in aerosol and cloud properties along the central California coast when winds change from northerly to southerly

Kira Zeider et al.

Correspondence to: Armin Sorooshian (armin@arizona.edu)

Section S1. Supplemental Discussion on Sect. 3.4.2

Complementary data from NAAPS and COAMPS are shown in Fig. S20 for this case flight. COAMPS and NAAPS (Fig. S20a and S20b, respectively) both show southerly winds generally in the outlined study domain, which is consistent with observational data showing southerly winds close to Marina. NAAPS shows stronger southerly winds over land near Marina compared to over Monterey Bay whereas there was not much of a difference in wind speed between the two spiral soundings from the Twin Otter (Fig. S19). COAMPS better simulates southerly flow along the coastline, whereas the spatial resolution of NAAPS is probably a reason for it not being able to capture southerly flow in the grid spaces closest to the coast especially just south of Marina – instead there is weak northerly flow.

Generally, NAAPS and COAMPS match in the areas identified as having smoke and areas of high concentrations match one another. There is a small difference between the two models with respect to smoke (Fig. S20c and S20d), as COAMPS more closely matches the visible satellite imagery from Fig. 8b. We do not focus on comparing absolute mass concentrations of smoke as it is difficult to know the ground truth value from the aircraft observations and also because of the different methods and size classifications for smoke in the two models. Looking at Fig. S20e, NAAPS shows high concentrations of sea salt offshore west of 130° W. However, near the flight area and within our region of focus, sea salt concentrations are less than 5 μg m^{-3}. NAAPS ABF (Fig. S20f) mirrors the areas with areas of high sea salt in Fig. 20e, but similar to model results from Sect. 3.2.2.4, there are areas of higher ABF concentrations (2 – 3 μg m^{-3}) near the ports of Los Angeles and Long Beach (34° N, 118° W) as well as up north near San Francisco and San Jose (38° N, 122° W). NAAPS dust (Fig. S20g) and coarse mass (Fig. S20h) also resemble the areas with high sea salt, with coarse mass concentrations exceeding 10 μg m^{-3} near both Marina, CA and Pt. Reyes.

Table S1: Median value (southerly/northerly) of various parameters over the ocean (without $N_{a>10nm}$ filtering). Mode values are used for wind direction. Refer to Table 3 caption for the airborne instruments that correspond to each parameter listed. The far right-hand columns indicate the number of data points (in the thousands) used from each campaign, with n_{Na} indicating the amount of data used for all N_a calculations, n_{Nd} is for cloud data, and n_{Wind} is for wind speed and direction. FSSP data were used for N_d data only during BOAS, whereas CASF was used in other campaigns. These data are for the lowest 800 m above sea level.

	$N_{a>10nm}$ (cm^{-3})	$N_{a10-100nm}$ (cm^{-3})	$N_{a0.1-1\mu m}$ (cm^{-3})	$N_{a>1\mu m}$ (cm^{-3})	N_{a3}:N_{a10} (-)	N_d (cm^{-3})	Wind Speed ($m\ s^{-1}$)	Wind Direction (°)	n_{Na} ($\times 10^3$)	n_{Nd} ($\times 10^3$)	n_{Wind} ($\times 10^3$)
E-PEACE	861 / 703	501 / 454	338 / 197	0 / 1.25	1.09 / 1.10	252 / 163	3.38 / 7.58	177.61 / 330.48	20.3 / 202.7	17.1 / 127.1	37.4 / 330.8
NiCE	953 / 775	248 / 329	471 / 326	2.51 / 1.25	1.12 / 1.19	249 / 255	3.80 / 4.75	180.81 / 327.20	1.4 / 78.6	1.5 / 39.7	3.0 / 124.8
BOAS	750 / 515	553 / 274	204 / 200	0 / 1.24	1.20 / 1.19	143 / 127	5.49 / 6.05	166.97 / 328.58	5.8 / 79.5	3.9 / 20.5	11.8 / 112.1
FASE	836 / 916	423 / 635	326 / 180	0 / 0	1.29 / 1.16	203 / 223	2.35 / 6.82	144.03 / 331.29	1.0 / 95.5	0.3 / 99.2	1.3 / 194.9
MACAWS	722 / 815	560 / 635	154 / 164	0 / 0	1.25 / 1.26	189 / 165	7.75 / 8.87	162.15 / 330.28	10.3 / 118.9	6.6 / 27.0	16.9 / 145.9
CSM	5,558 / 3,451	5,081 / 3,366	515 / 365	1.00 / 0	1.30 / 1.67	334 / 314	6.10 / 6.77	193.93 / 332.16	4.8 / 31.5	1.8 / 4.1	6.9 / 41.3

Table S2: Median value (southerly/northerly) of various parameters for individual campaigns in the region of focus (over land and ocean; without $N_{a>10nm}$ filtering). Mode values are used for wind direction. Refer to Table 3 caption for the airborne instruments that correspond to each parameter listed. The far right-hand columns indicate the number of data points (in the thousands) used from each campaign, with n_{Na} indicating the amount of data used for all N_a calculations, n_{Nd} is for cloud data, and n_{Wind} is for wind speed and direction. FSSP data were used for N_d data only during BOAS, whereas CASF was used in other campaigns. These data are for the lowest 800 m above sea level.

	$N_{a>10nm}$ (cm^{-3})	$N_{a10-100nm}$ (cm^{-3})	$N_{a0.1-1\mu m}$ (cm^{-3})	$N_{a>1\mu m}$ (cm^{-3})	$N_{a3}:N_{a10}$ (-)	N_d (cm^{-3})	Wind Speed ($m\ s^{-1}$)	Wind Direction (°)	n_{Na} ($\times 10^3$)	n_{Nd} ($\times 10^3$)	n_{Wind} ($\times 10^3$)
E-PEACE	861 / 725	501 / 473	338 / 201	0 / 0	1.9 / 1.10	252 / 163	3.38 / 6.24	177.61 / 330.48	20.3 / 210.7	17.1 / 127.1	37.5 / 408.4
NiCE	11,900 / 2,030	10,095 / 1,564	1,399 / 603	1.30 / 1.26	1.50 / 1.31	250 / 253	3.38 / 3.95	160.65 / 327.20	5.4 / 158.1	1.6 / 42.1	27.4 / 241.1
BOAS	1,337 / 534	909 / 302	243 / 207	0 / 0	1.21 / 1.20	143 / 127	5.28 / 5.27	166.11 / 328.58	7.8 / 98.4	4.0 / 20.6	14.5 / 156.4
FASE	1,295 / 928	636 / 640	280 / 182	0 / 0	1.39 / 1.16	203 / 224	3.17 / 6.97	144.03 / 331.29	1.7 / 97.8	0.3 / 100.3	2.1 / 218.6
MACAWS	722 / 931	560 / 737	154 / 169	0 / 0	1.25 / 1.28	189 / 165	7.69 / 7.64	162.15 / 330.28	10.3 / 136.5	6.6 / 27.1	18.2 / 193.7
CSM	5,015 / 2,507	4.573 / 2,047	529 / 405	1.00 / 0	1.33 / 1.53	334 / 314	5.86 / 4.94	193.93 / 329.31	4.9 / 22.1	1.8 / 4.1	8.6 / 52.5

Table S3: Median value (southerly/northerly) of various parameters for individual campaigns in the region of focus (over land and ocean) with a $N_{a>10nm}$ filter. RFs with median $N_{a>10nm}$ > 7,000 cm^{-3} were removed from the final analysis to eliminate smoke interference. Mode values are used for wind direction. Refer to Table 3 caption for the airborne instruments that correspond to each parameter listed. The far right-hand columns indicate the number of data points (in the thousands) used from each campaign, with n_{Na} indicating the amount of data used for all N_a calculations, n_{Nd} is for cloud data, and n_{Wind} is for wind speed and direction. FSSP data were used for N_d data only during BOAS, whereas CASF was used in other campaigns. These data are for the lowest 800 m above sea level.

	$N_{a>10nm}$ (cm^{-3})	$N_{a10-100nm}$ (cm^{-3})	$N_{a0.1-1\mu m}$ (cm^{-3})	$N_{a>1\mu m}$ (cm^{-3})	N_{a3}:N_{a10} (-)	N_d (cm^{-3})	Wind Speed ($m\ s^{-1}$)	Wind Direction (°)	n_{Na} ($\times 10^3$)	n_{Nd} ($\times 10^3$)	n_{Wind} ($\times 10^3$)
E-PEACE	861 / 725	338 / 201	501 / 473	0 / 0	1.09 / 1.10	252 / 163	3.38 / 6.24	177.61 / 330.48	20.3 / 210.7	17.1 / 127.1	37.5 / 408.4
NiCE	1,060 / 778	519 / 319	351 / 309	1.30 / 0	1.15 / 1.18	250 / 254	4.02 / 5.08	197.78 / 327.20	1.9 / 81.2	1.6 / 41.5	18.5 / 150.7
BOAS	1,337 / 522	243 / 200	909 / 285	0 / 0	1.21 / 1.20	143 / 127	5.28 / 5.47	166.11 / 328.58	7.8 / 90.8	3.9 / 20.6	14.5 / 148.9
FASE	1,295 / 926	280 / 182	636 / 639	0 / 0	1.39 / 1.16	203 / 224	3.17 / 6.99	144.03 / 331.29	1.7 / 97.4	0.3 / 100.3	2.1 / 218.2
MACAWS	722 / 794	154 / 166	560 / 617	0 / 0	1.25 / 1.26	189 / 165	7.69 / 7.90	162.15 / 330.28	10.3 / 122.2	6.6 / 27.1	18.2 / 179.1
CSM	5,015 / 4,795	529 / 417	4,572 / 4,130	1.00 / 0	1.33 / 1.63	334 / 314	3.38 / 5.03	177.61 / 329.31	4.9 / 29.1	1.8 / 4.1	37.5 / 59.5

Table S4: Mann-Whitney U test results (p-values) of airborne data from Table 3 (ocean-only and filtered to remove smoke). Box plots of these variables are found in Fig. S10. The null hypotheses ($p \leq 0.05$) for this test were that southerly and northerly wind days had similar N_a, N_d, and wind medians within a campaign.

	$N_{a>10nm}$	$N_{a10-100nm}$	$N_{a0.1-1\mu m}$	$N_{a>1\mu m}$	N_{a3}:N_{a10}	N_d	Wind Speed	Wind Direction
E-PEACE	4.26 (E-299)	2.10 (E-57)	0.00	0.00	1.54 (E-32)	0.00	0.00	0.00
NiCE	2.19 (E-51)	0.04	2.15 (E-73)	9.12 (E-146)	3.57 (E-23)	1.22 (E-3)	1.57 (E-76)	0.00
BOAS	0.00	0.00	5.52 (E-52)	0.00	1.55 (E-37)	1.49 (E-3)	2.34 (E-184)	0.00
FASE	5.54 (E-5)	7.97 (E-33)	3.45 (E-87)	2.74 (E-7)	5.49 (E-179)	7.65 (E-7)	1.84 (E-111)	0.00
MACAWS	3.36 (E-63)	2.67 (E-67)	0.94	0.00	1.65 (E-57)	1.16 (E-163)	0.00	0.00
CSM	0.00	8.52 (E-113)	0.00	2.00 (E-241)	7.62 (E-49)	4.99 (E-25)	1.27 (E-71)	0.00

Table S5: Mann-Whitney U test results (p-values) of cloud water data from Table 4 (ocean-only and filtered to remove smoke). Box plots of these variables are found in Fig. S11. CSM did not deploy a cloud water collector. The null hypothesis ($p \leq 0.05$) for this test was that southerly and northerly wind days had similar median concentrations for the selected species. There is no NH_4^+ p-value for E-PEACE because there was no NH_4^+ data for that campaign, and there is no V p-value for BOAS because there was no valid data for southerly wind days to compare to northerly wind days.

	Ca^{2+}	Cl^-/Na^+	K^+	Na^+	NH_4^+	NO_3^-	Oxalate	pH	nss-SO_4^{2-}	V
E-PEACE	0.45	1.03 (E-3)	0.02	0.01	—	1.73 (E-6)	0.74	6.60 (E-5)	1.52 (E-3)	4.25 (E-7)
NiCE	0.16	0.01	0.04	0.08	0.79	0.40	0.12	0.17	0.19	0.91
BOAS	1.00	0.09	1.00	0.90	0.04	0.01	0.04	0.40	0.90	—
FASE	0.68	0.80	0.37	0.77	0.40	0.80	0.49	0.54	0.60	0.89
MACAWS	0.07	0.24	0.49	0.69	0.06	0.09	1.06 (E-3)	0.01	0.96	0.10

Table S6: Median mass concentrations (µg m^{-3}) of selected IMPROVE species for southerly and northerly wind days (number of days in parentheses) during E-PEACE and BOAS (other campaigns omitted due to low number (< 2) of valid southerly wind days): Cl^-, elemental carbon (EC), fine soil, K^+, Ni, NO_3^-, organic carbon (OC), particulate matter with diameter less than 2.5 µm ($PM_{2.5}$), coarse mass ($PM_{coarse} = PM_{10} - PM_{2.5}$), Si, SO_4^{2-}, and V. Ni, Si, and V (*) are reported in ng m^{-3}. Additionally listed are p-values calculated from a Mann-Whitney U test for each species during the individual campaigns. The null hypothesis ($p \leq 0.05$) for the tests was that southerly and northerly wind days had similar median species concentrations.

	Cl^-	EC	Fine Soil	K^+	Ni	NO_3^-	OC	$PM_{2.5}$	PM_{coarse}	Si	SO_4^{2-}	V
E-PEACE												
Southerly (3)	0.56	0.02	0.04	0.01	0.20*	0.27	0.22	3.39	3.18	1.67*	1.36	1.56*
Northerly (18)	0.68	0.01	0.04	0.02	0.17*	0.11	0.20	3.78	4.21	2.40*	0.92	0.58*
p-value	0.96	0.42	0.81	0.89	0.18	0.20	0.67	0.81	0.81	0.53	0.23	0.02
BOAS												
Southerly (2)	1.07	0.02	0.12	0.04	0.12*	0.34	0.36	7.61	6.74	8.29*	1.01	0.09*
Northerly (7)	0.65	0.02	0.08	0.02	0.02*	0.10	0.25	4.82	3.60	2.61*	0.67	0.11*
p-value	0.60	0.79	0.30	0.60	0.07	0.04	0.19	0.60	0.60	0.07	0.12	0.79

Table S7: Median values (southerly/northerly) of MODIS parameters for individual campaigns, including cloud effective particle radius (r_e; µm), cloud liquid water path (LWP; g m^{-2}), cloud optical thickness (COT), cloud fraction (from cloud mask), and aerosol optical depth (AOD, combined dark target and deep blue at 0.55 µm for land and ocean). The spatial area of analysis was bounded by 35.31° N – 40.99° N, 125.93° W – 118.98° W. N_d (cm^{-3}) was calculated from MODIS properties based on Eq. 3. The far right-hand column (n) indicates the number of daily mean values used in each campaign.

	Cloud LWP (g m^{-2})	COT	Cloud r_e (µm)	Cloud fraction	AOD	N_d (cm^{-3})	n
E-PEACE	66.48 / 67.17	10.27 / 8.42	9.94 / 11.97	0.47 / 0.44	0.10 / 0.09	138.54 / 91.99	8 / 44
NiCE	82.78 / 74.54	10.52 / 9.93	11.47 / 11.78	0.53 / 0.49	0.24 / 0.12	112.18 / 103.09	9 / 46
BOAS	84.40 / 89.90	11.88 / 10.87	11.77 / 13.29	0.58 / 0.57	0.12 / 0.11	96.59 / 72.80	8 / 17
FASE	87.12 / 75.94	11.49 / 10.28	12.00 / 11.32	0.43 / 0.48	0.19 / 0.12	96.37 / 99.16	9 / 41
MACAWS	101.47 / 65.10	12.31 / 8.97	12.55 / 11.17	0.74 / 0.47	0.16 / 0.14	88.28 / 102.14	2 / 41
CSM	74.24 / 52.50	7.56 / 6.12	15.02 / 14.16	0.57 / 0.44	2.54 / 0.58	47.29 / 48.26	3 / 14

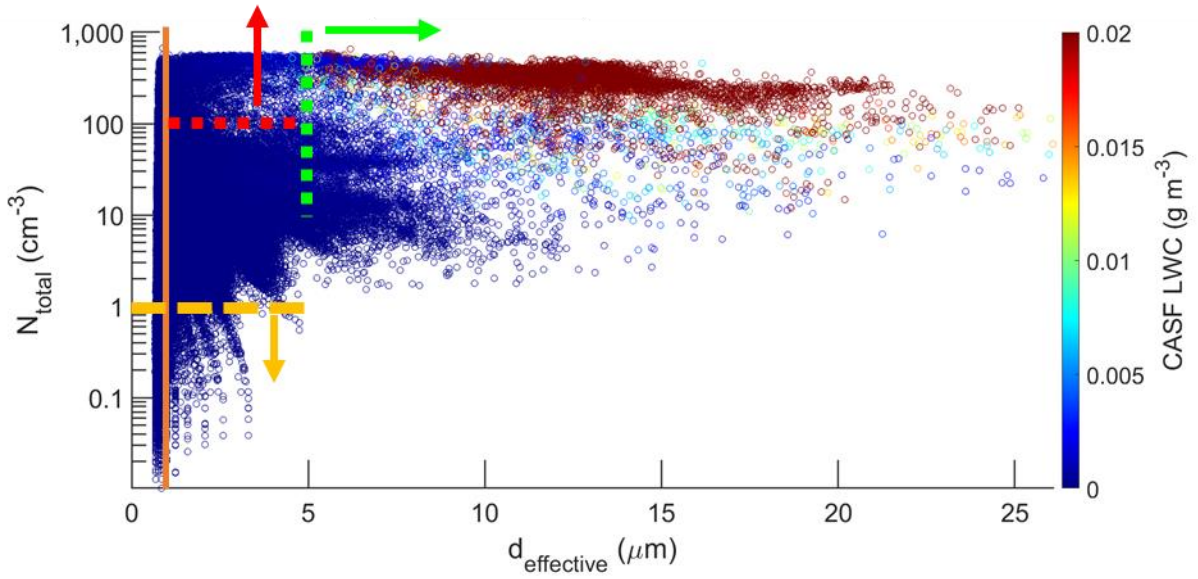

Figure S1: Scatterplot of N_{total} (cm^{-3}) versus $d_{effective}$ (µm) from CASF for the CSM campaign. Points are colored by LWC from CASF ($g\ m^{-3}$). The data points with LWC > 0.02 $g\ m^{-3}$ and higher $d_{effective}$ indicate cloud water drops (suggested by the dotted green line and arrow at ~ 5 µm). The orange line indicates a $d_{effective}$ of 1 µm, the dashed yellow line and arrow suggest where mostly sea salt particles would be, and the dashed red line and arrow indicate coarse particles associated with smoke plumes. This analysis is relevant to the other campaigns in terms of showing that a LWC threshold of 0.02 $g\ m^{-3}$ is adequate for identifying when the aircraft was in cloud.

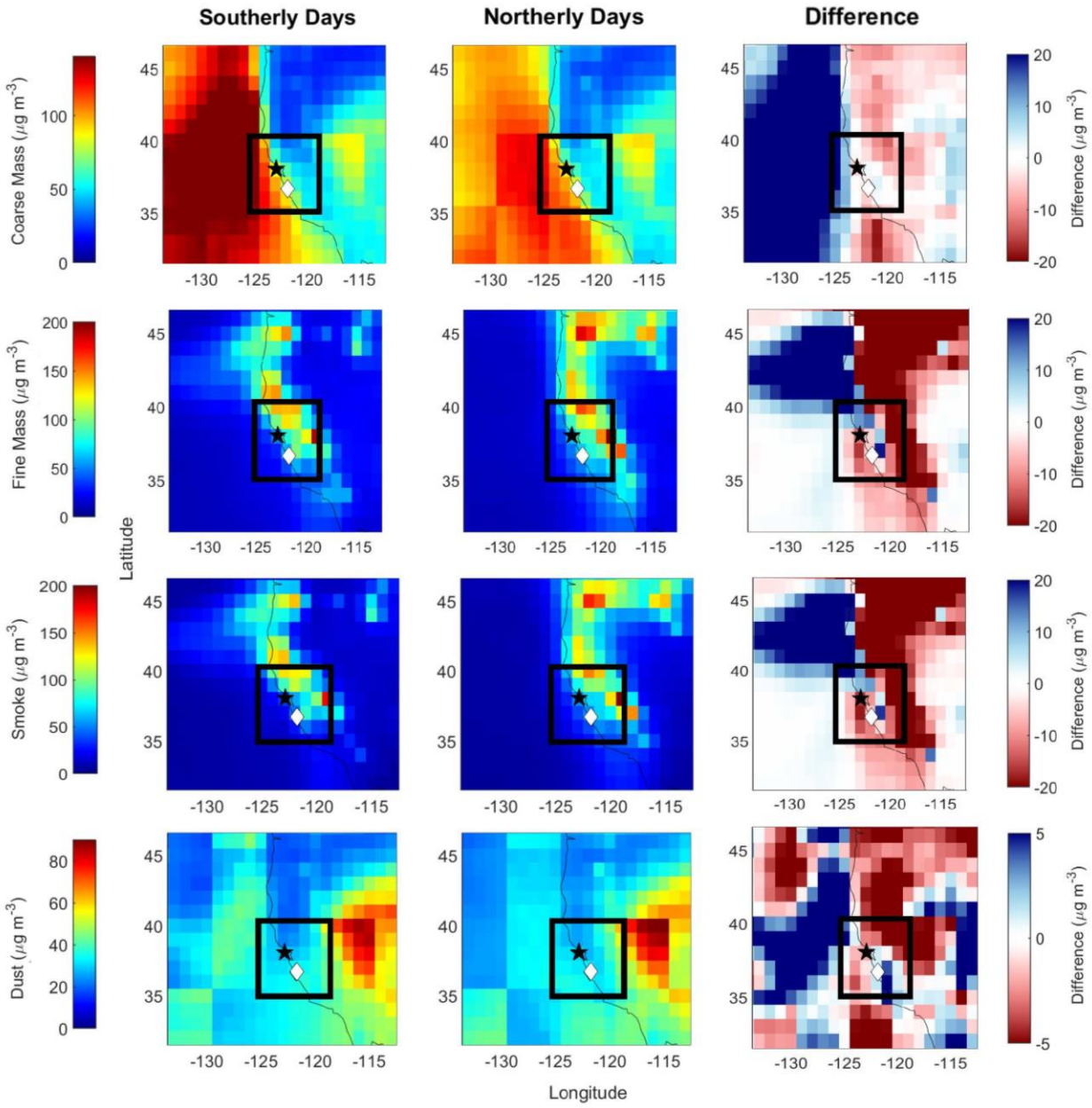

Figure S2: Total fine mass, coarse mass, smoke, and dust concentrations (μg m^{-3}) of campaign months at 1800 UTC for 1st through 5th NAAPS levels (up to ~668 m above sea level) for southerly and northerly wind days. The right-most panel illustrates the difference between southerly and northerly wind days. The airport in Marina, CA is denoted by a white diamond, Pt. Reyes is indicated with a black star, and the black box indicates the region of focus in this study.

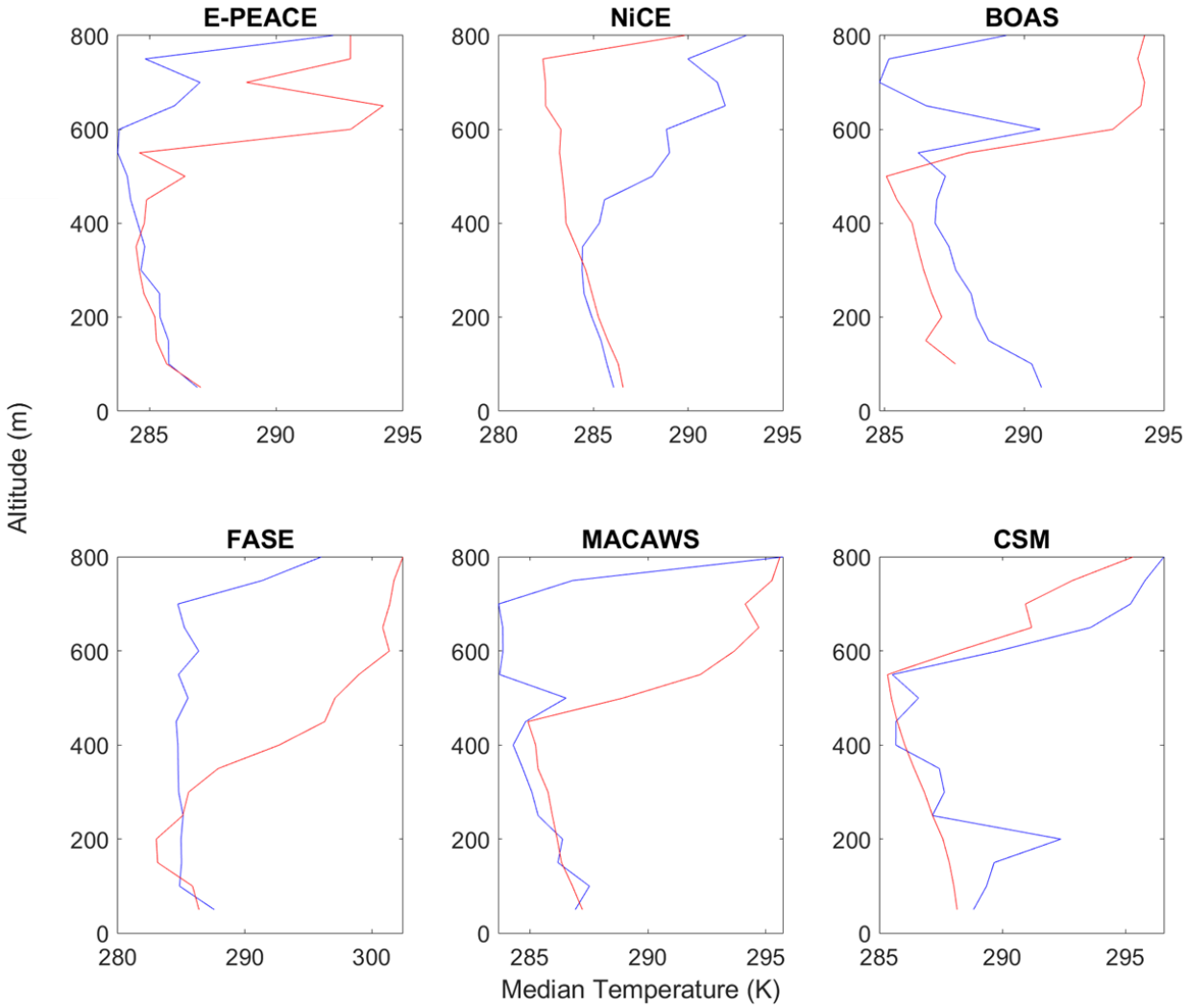

Figure S3: Median temperature vertical distributions for each campaign (northerly = blue; southerly = red). These data are based on aircraft measurements and are only over the ocean and screened to omit wildfire influence using criterion mentioned in Sect. 2.1.

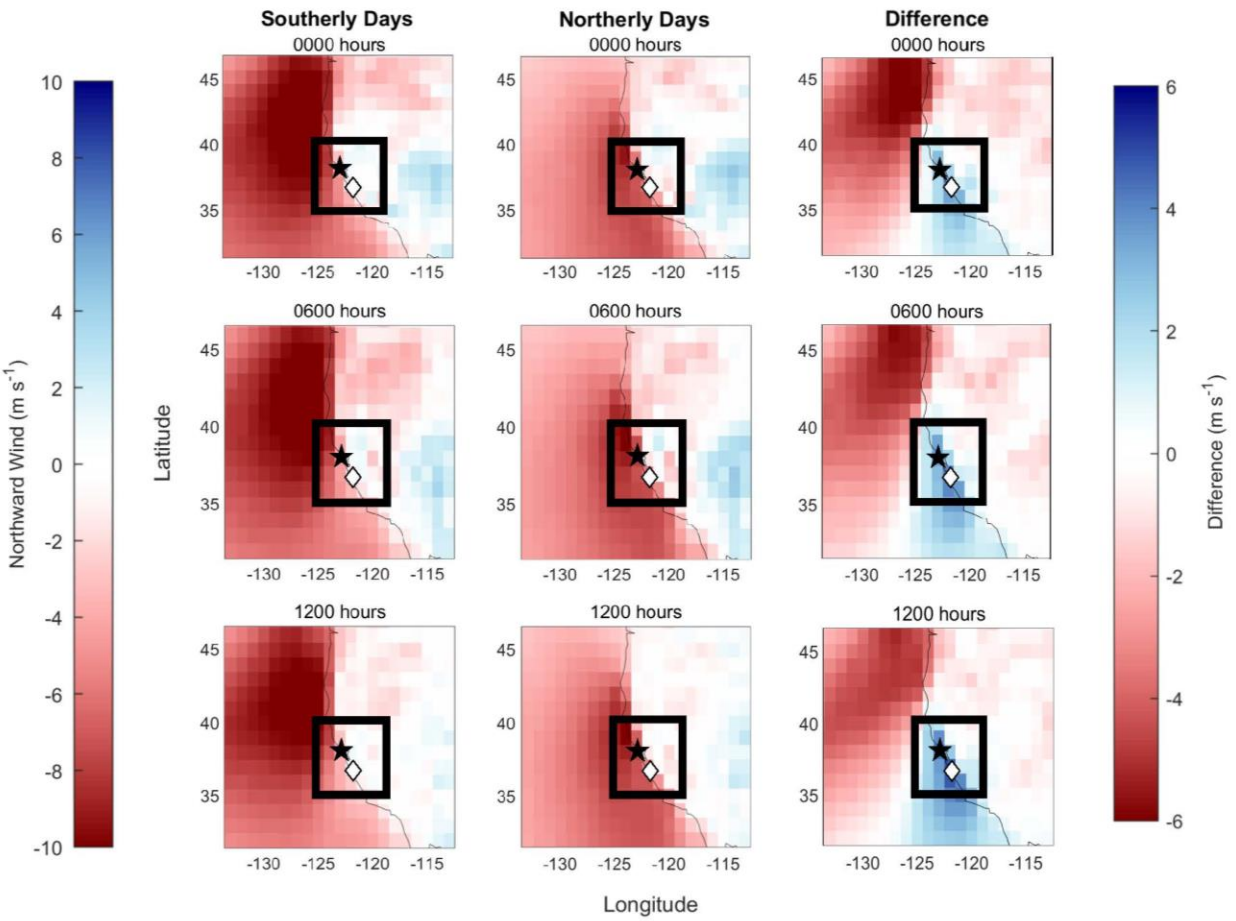

Figure S4: Average northward wind speed (v_{wind}: m s^{-1}) of campaign months (see Table 1) at 0000, 0600, and 1200 UTC for 1st through 5th NAAPS levels (up to ~668 m above sea level) for days identified as having southerly and northerly wind based on datasets described in Section 2.2. The color bar for the left two columns of panels can be interpreted as red values being for northerly flow and blue as southerly flow. The right-most panel illustrates the difference between southerly and northerly wind days. The airport in Marina, California is denoted by a white diamond, Pt. Reyes is indicated with a black star, and the black box outlines the region of focus in this study.

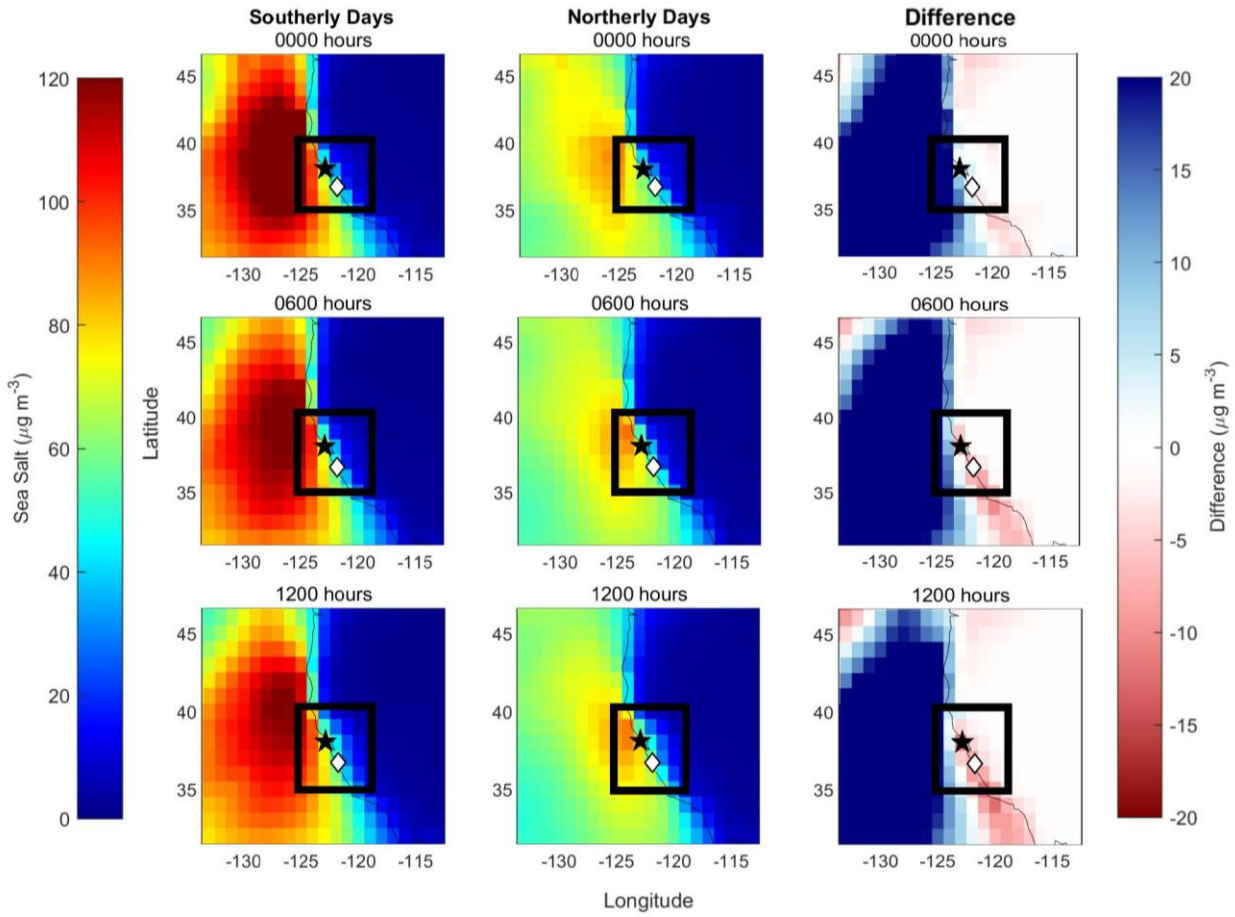

Figure S5: Total sea salt mass concentration (μg m^{-3}) of campaign months at 0000, 0600, and 1200 UTC 1st through 5th NAAPS levels (up to ~668 m above sea level) for days identified as having southerly and northerly wind based on datasets described in Section 2.2. The right-most panel illustrates the difference between southerly and northerly wind days. The airport in Marina, California is denoted by a white diamond, Pt. Reyes is indicated with a black star, and the black box indicates the region of focus in this study.

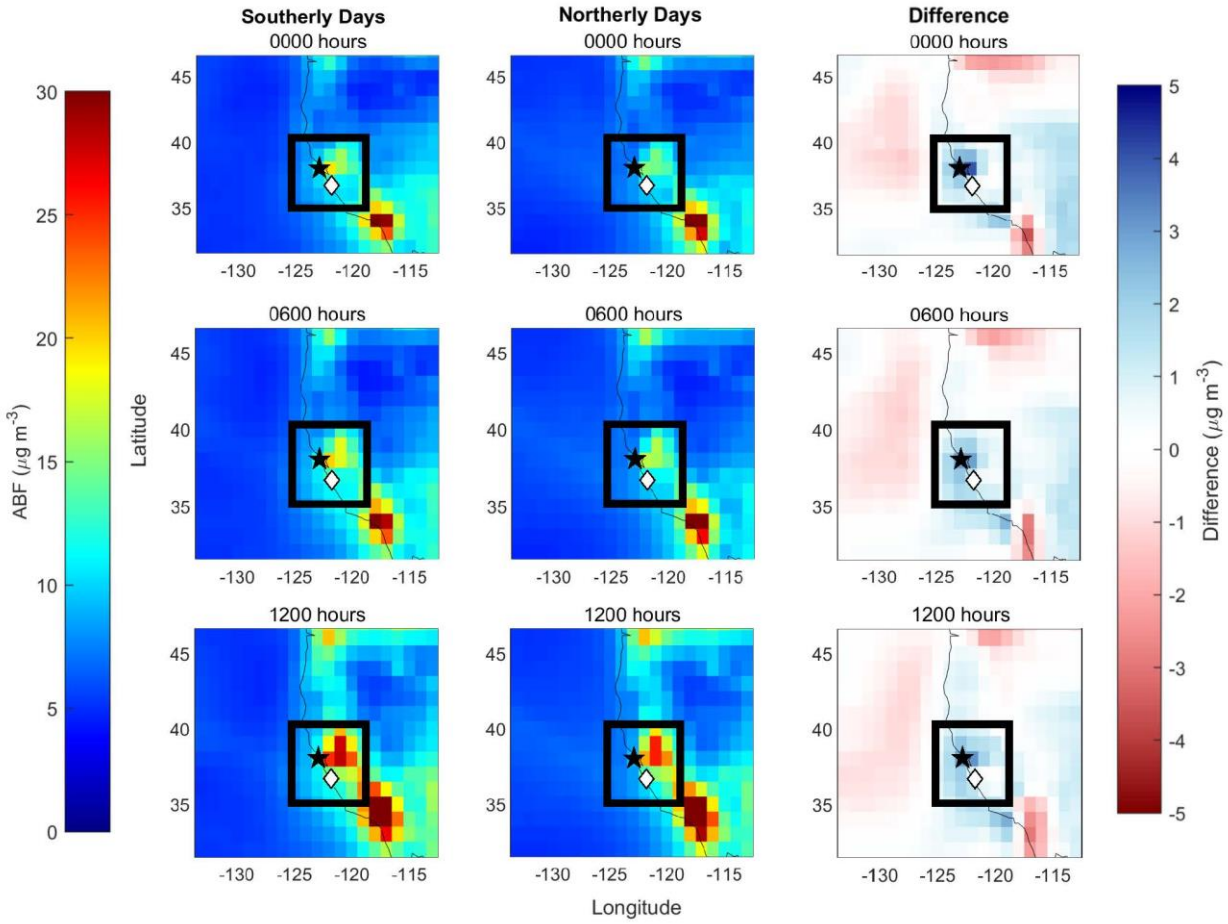

Figure S6: Total anthropogenic and biogenic fine (ABF) aerosol mass concentration (μg m^{-3}) of campaign months at 0000, 0600, and 1200 UTC 1st through 5th NAAPS levels (up to ~668 m above sea level) for days identified as having southerly and northerly wind based on datasets described in Section 2.2. The right-most panel illustrates the difference between southerly and northerly wind days. The airport in Marina, California is denoted by a white diamond, Pt. Reyes is indicated with a black star, and the black box indicates the region of focus in this study.

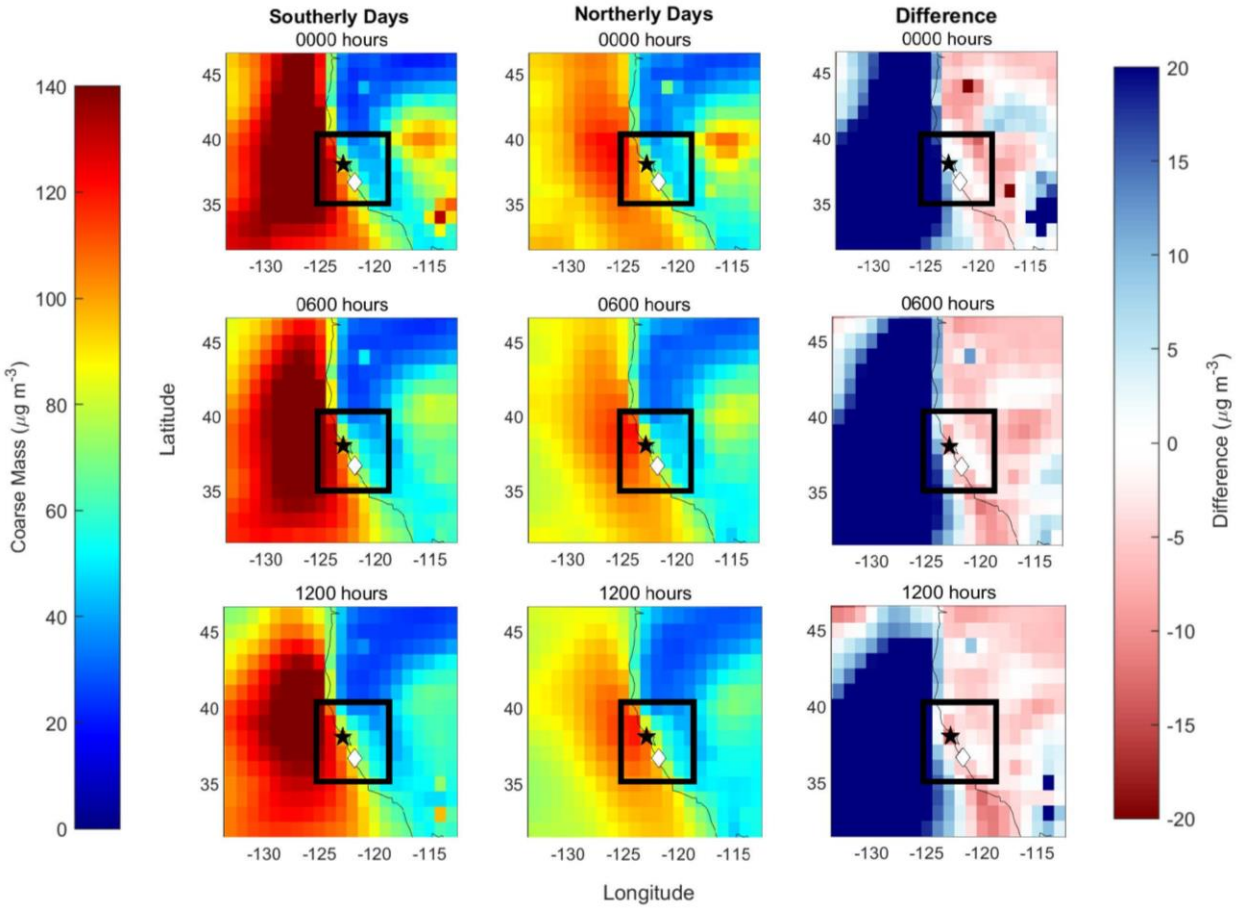

Figure S7: Total coarse mass concentration (μg m^{-3}) of campaign months at 0000, 0600, and 1200 UTC 1st through 5th NAAPS levels (up to ~668 m above sea level) for days identified as having southerly and northerly wind based on datasets described in Section 2.2. The right-most panel illustrates the difference between southerly and northerly wind days. The airport in Marina, California is denoted by a white diamond, Pt. Reyes is indicated with a black star, and the black box indicates the region of focus in this study.

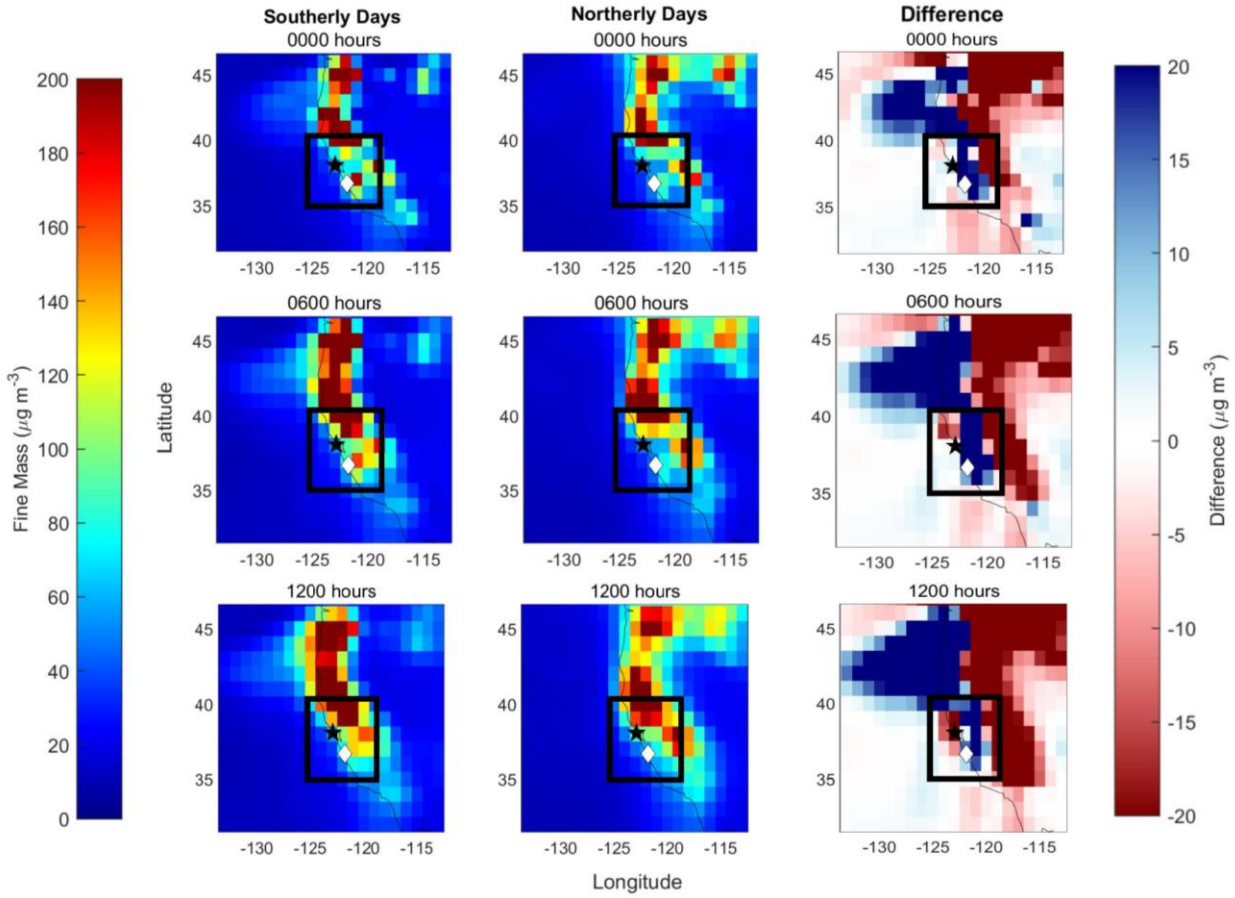

Figure S8: Total fine mass concentration (μg m^{-3}) of campaign months at 0000, 0600, and 1200 UTC 1st through 5th NAAPS levels (up to ~668 m above sea level) for days identified as having southerly and northerly wind based on datasets described in Section 2.2. The right-most panel illustrates the difference between southerly and northerly wind days. The airport in Marina, California is denoted by a white diamond, Pt. Reyes is indicated with a black star, and the black box indicates the region of focus in this study.

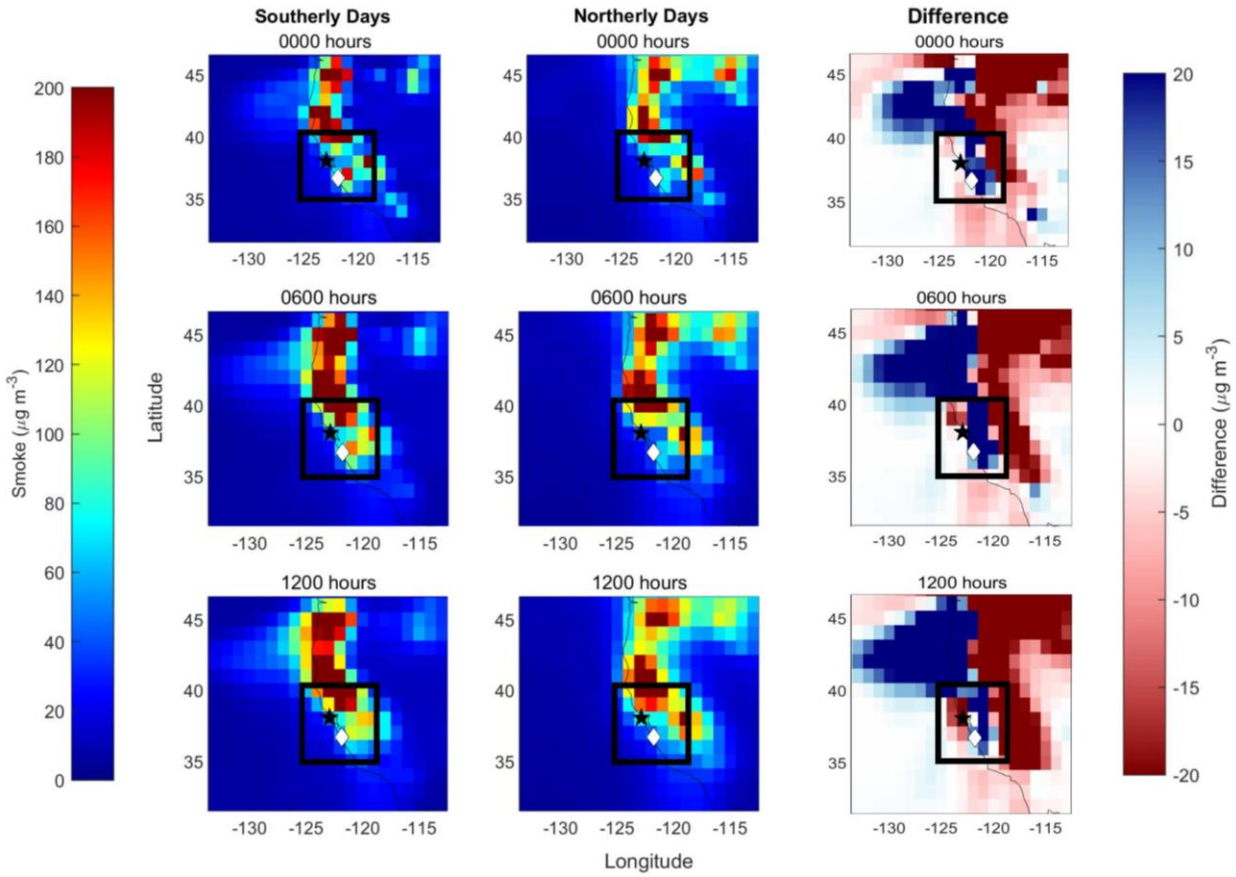

Figure S9: Total smoke mass concentration (μg m^{-3}) of campaign months at 0000, 0600, and 1200 UTC 1st through 5th NAAPS levels (up to ~668 m above sea level) for days identified as having southerly and northerly wind based on datasets described in Section 2.2. The right-most panel illustrates the difference between southerly and northerly wind days. The airport in Marina, California is denoted by a white diamond, Pt. Reyes is indicated with a black star, and the black box indicates the region of focus in this study.

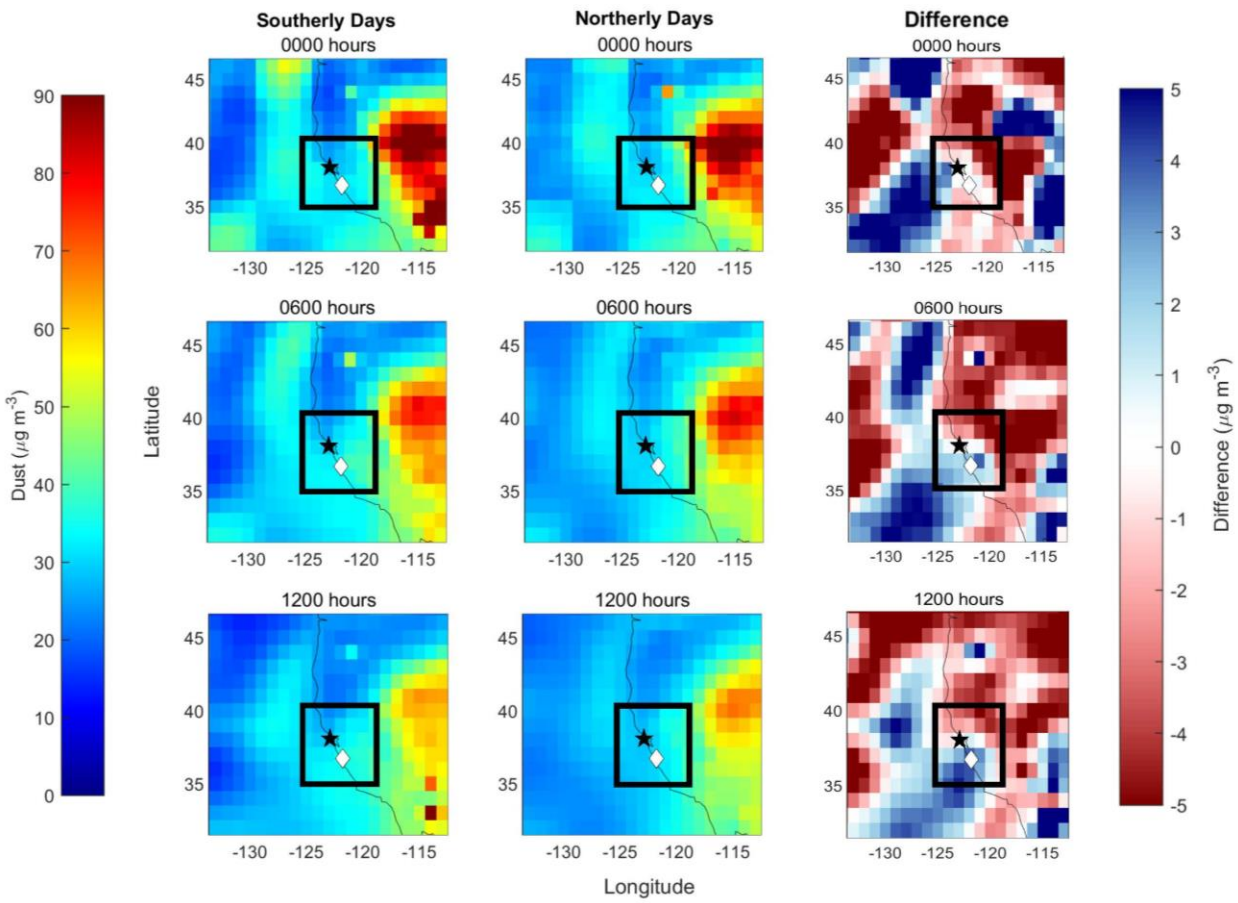

Figure S10: Total dust mass concentration (μg m^{-3}) of campaign months at 0000, 0600, and 1200 UTC 1st through 5th NAAPS levels (up to ~668 m above sea level) for days identified as having southerly and northerly wind based on datasets described in Section 2.2. The right-most panel illustrates the difference between southerly and northerly wind days. The airport in Marina, California is denoted by a white diamond, Pt. Reyes is indicated with a black star, and the black box indicates the region of focus in this study.

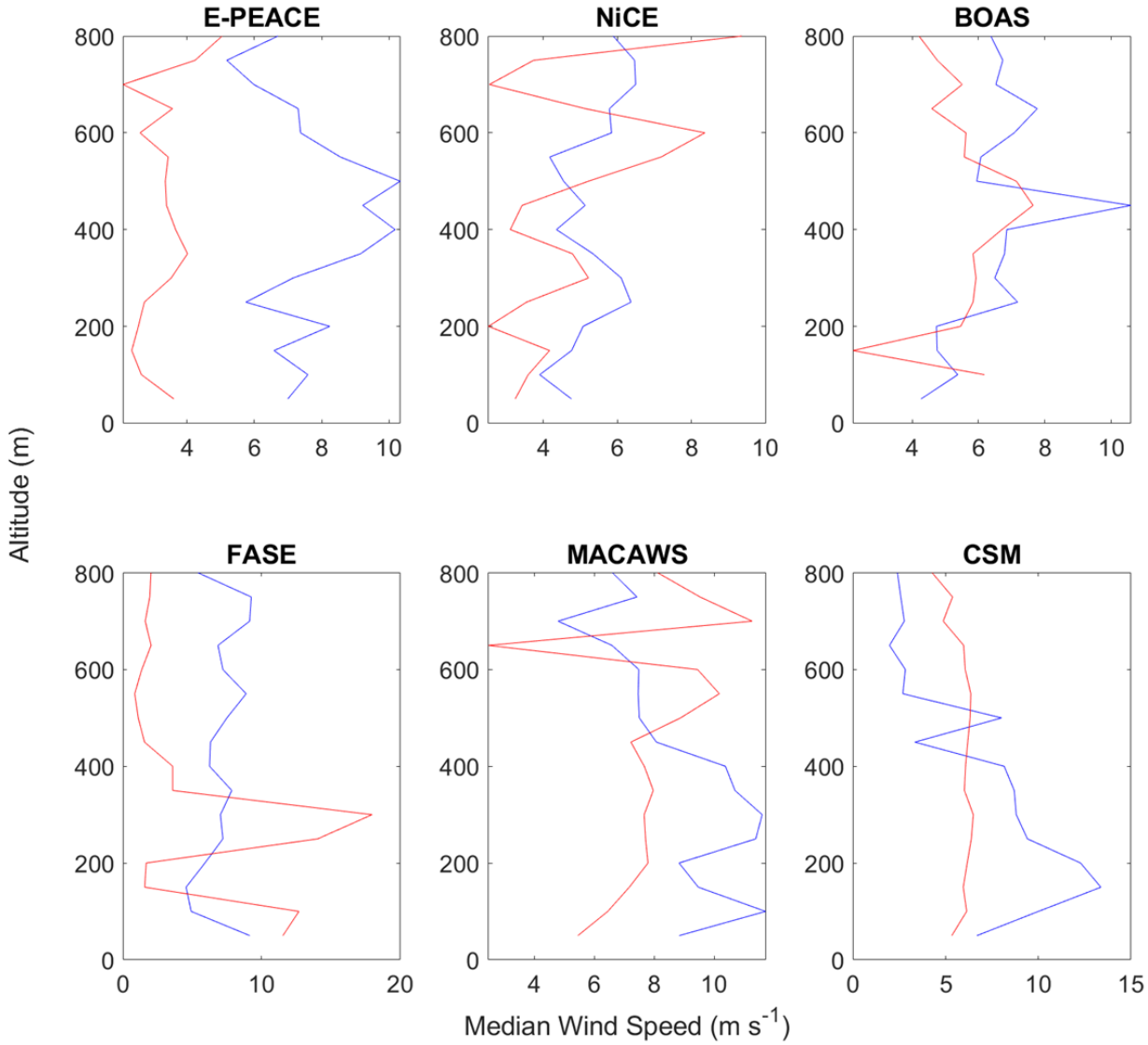

Figure S11: Median vertical wind speed profiles for each campaign (northerly = blue; southerly = red). These data are based on aircraft measurements and are only over the ocean and screened to omit wildfire influence using criterion mentioned in Sect. 2.1.

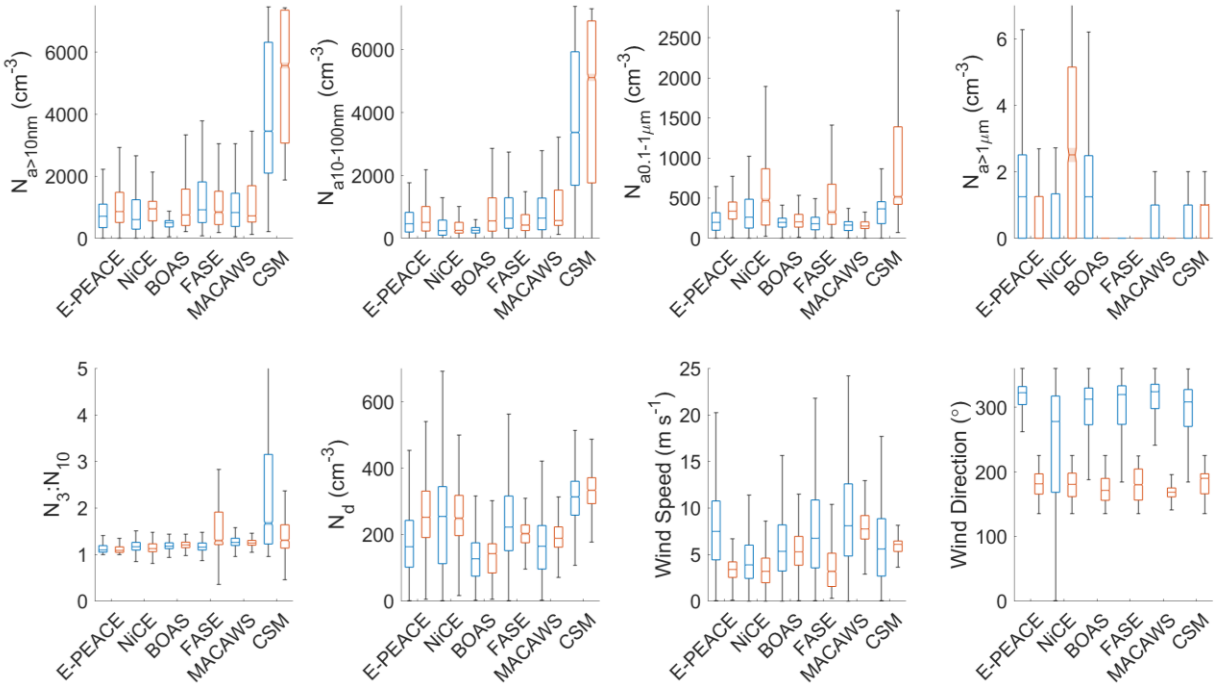

Figure S12: Box plots of airborne data (Table 3) over the ocean in the study region during each campaign after removal of data when a flight's median $N_{a>10nm}$ exceeded 7,000 cm^{-3}. Northerly and southerly data are represented by blue and red boxes, respectively. The notches (and shading) of the boxes assist in the determination of significance between multiple medians. The p-values derived from Mann-Whitney U tests are reported in Table S4.

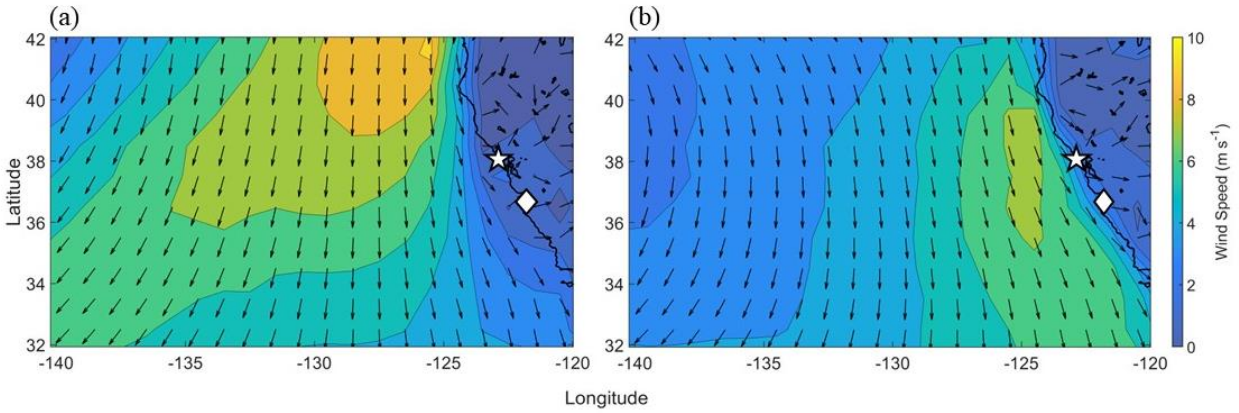

Figure S13: NAVGEM boundary layer flow patterns for (a) all southerly flow days and (b) all northerly flow days included in this study. These results are for 1800 UTC for all days of the campaign months in Table 1 as was done for Figs. S4-S10; the lowest level of the model was used representing the lowest ~50 m. The airport in Marina, California is denoted by a white diamond and Pt. Reyes is indicated with a white star.

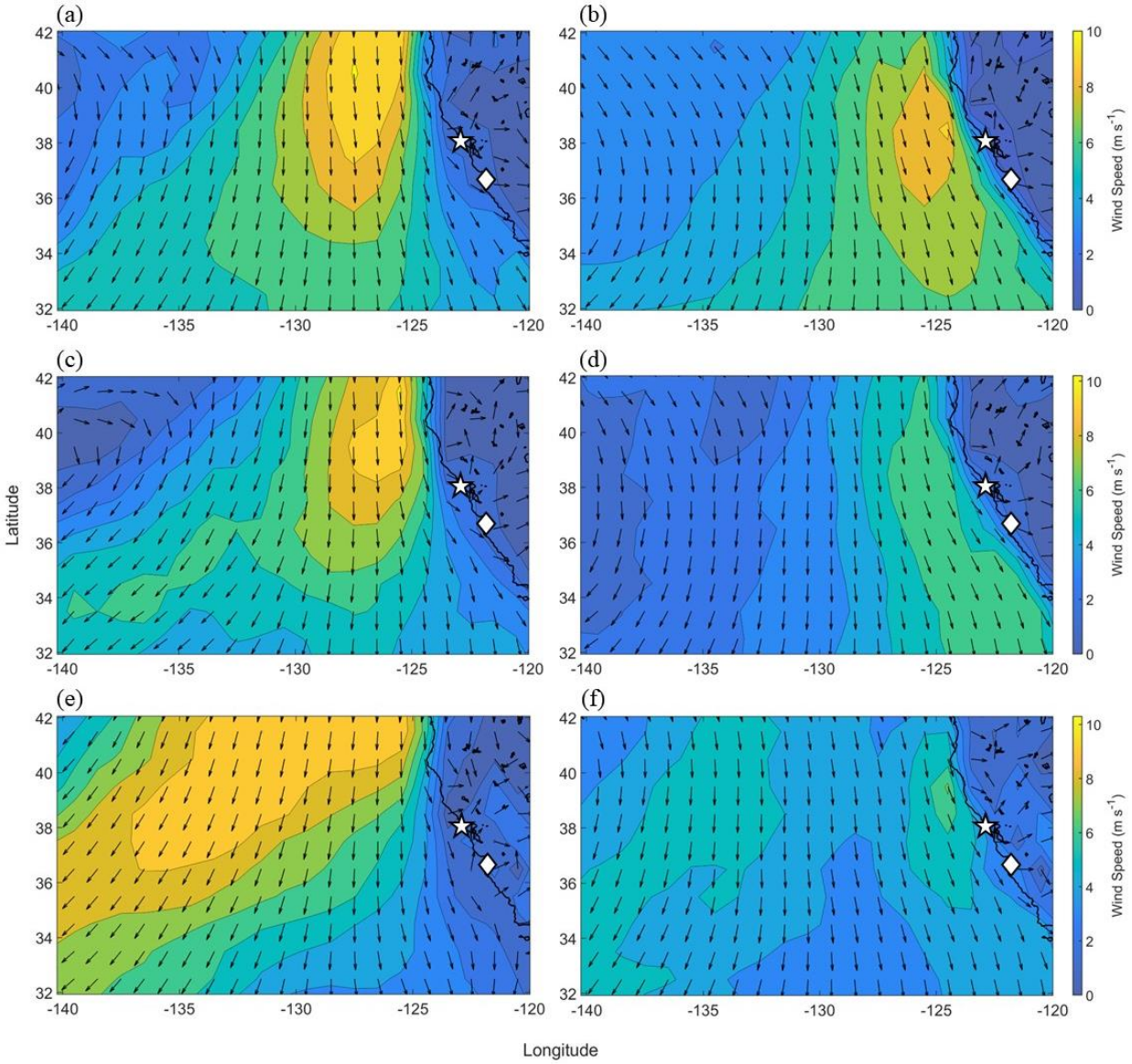

Figure S14: NAVGEM boundary layer flow patterns for (left) southerly and (right) northerly flow days during (a-b) E-PEACE, (c-d) NiCE, and (e-f) BOAS. These results are for 1800 UTC for all days of these respective campaign months in Table 1; the lowest level of the model was used representing the lowest ~50 m. The airport in Marina, California is denoted by a white diamond and Pt. Reyes is indicated with a white star.

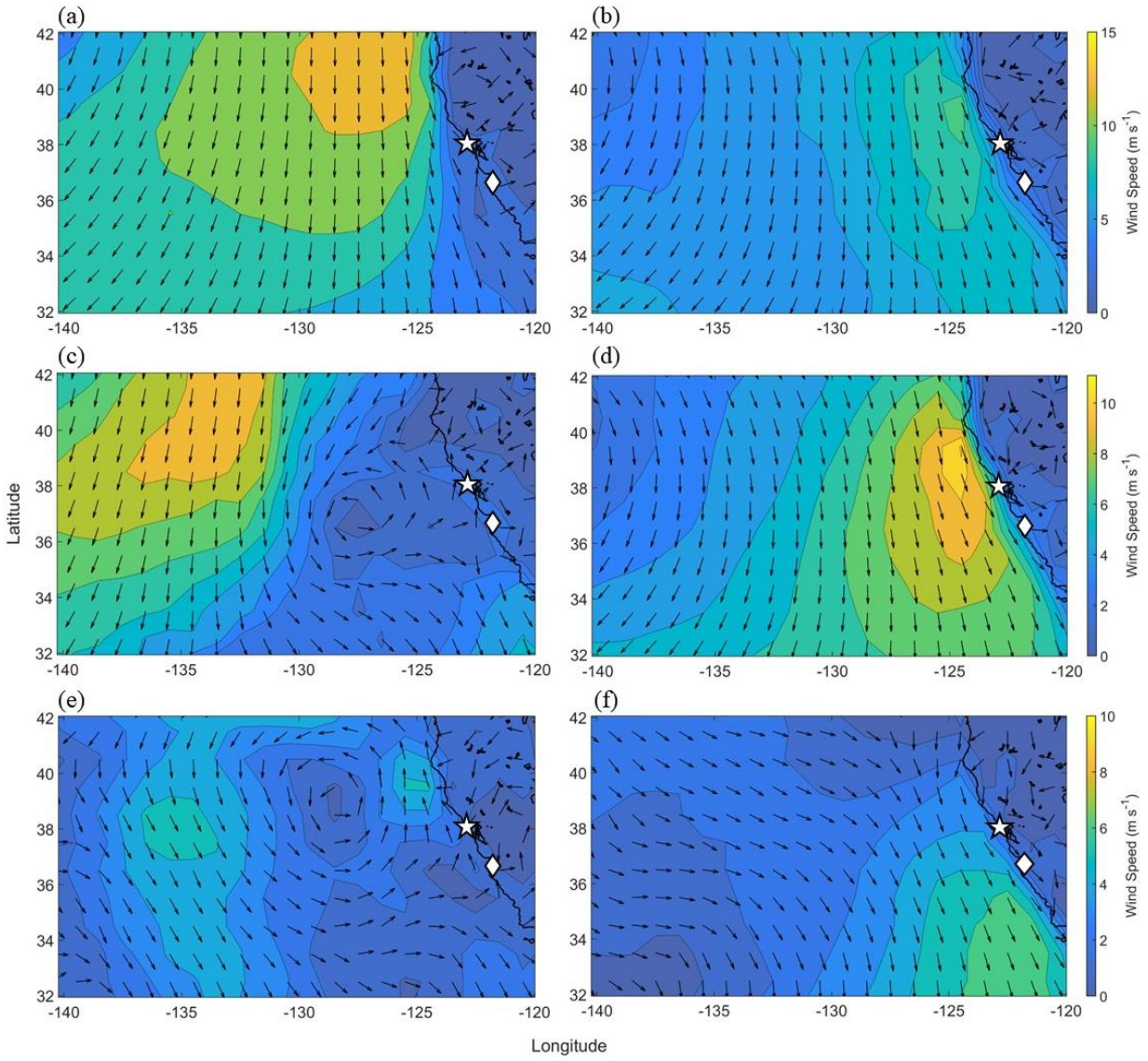

Figure S15: NAVGEM boundary layer flow patterns for (left) southerly and (right) northerly flow days during (a-b) FASE, (c-d) MACAWS, and (e-f) CSM. These results are for 1800 UTC for all days of these respective campaign months in Table 1; the lowest level of the model was used representing the lowest ~50 m. The airport in Marina, California is denoted by a white diamond and Pt. Reyes is indicated with a white star.

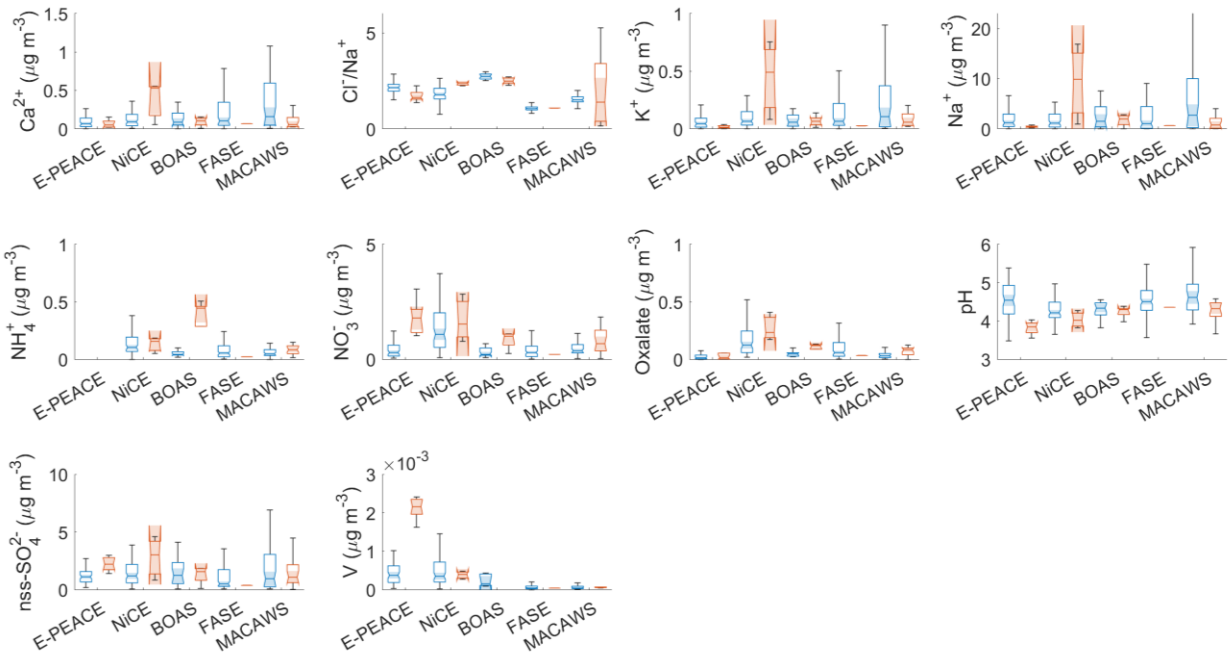

Figure S16: Box plots of cloud water speciated concentrations, along with Cl^-:Na^+ mass ratio and pH, within the study region during each campaign. The northerly data are represented by the blue boxes, and the southerly data are represented by the red boxes. The notches (and shading) of the boxes assist in the determination of significance between multiple medians. The p-values derived from Mann-Whitney U tests are reported in Table S5. No cloud water data are available for CSM.

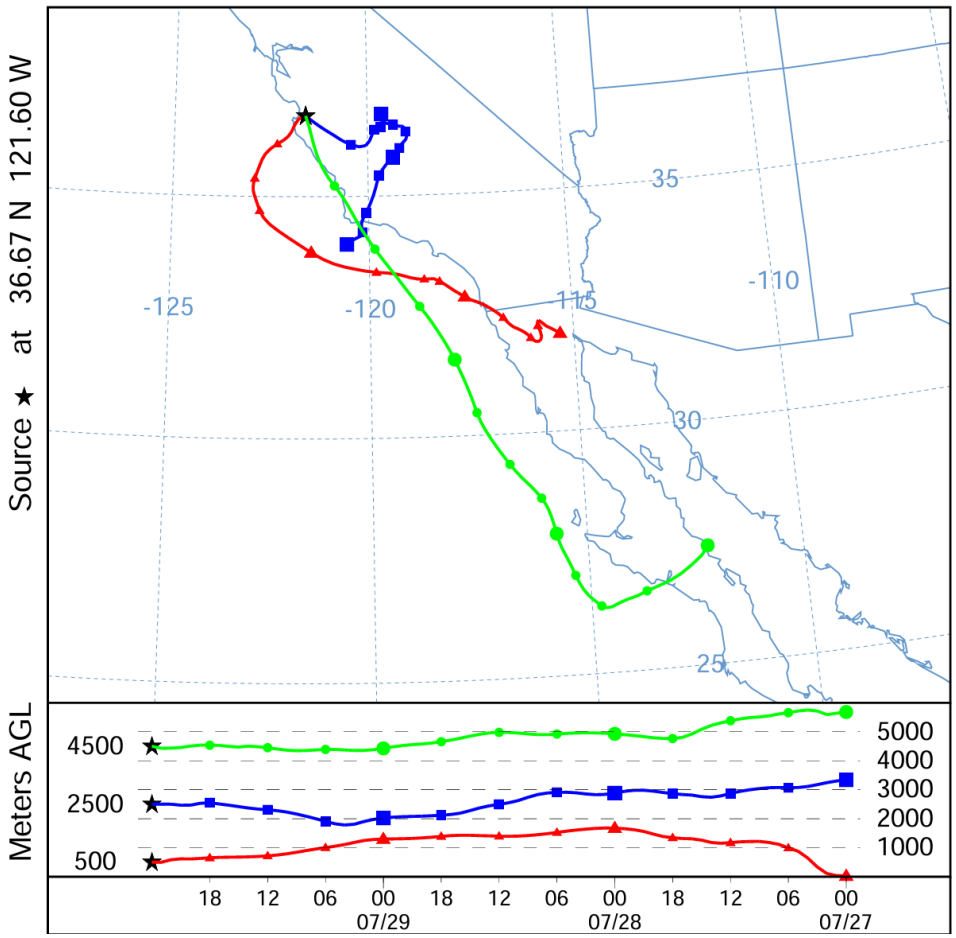

Figure S17: 72-hour HYSPLIT back-trajectory ending on 30 July 2018 by Marina, CA (indicated by the black star).

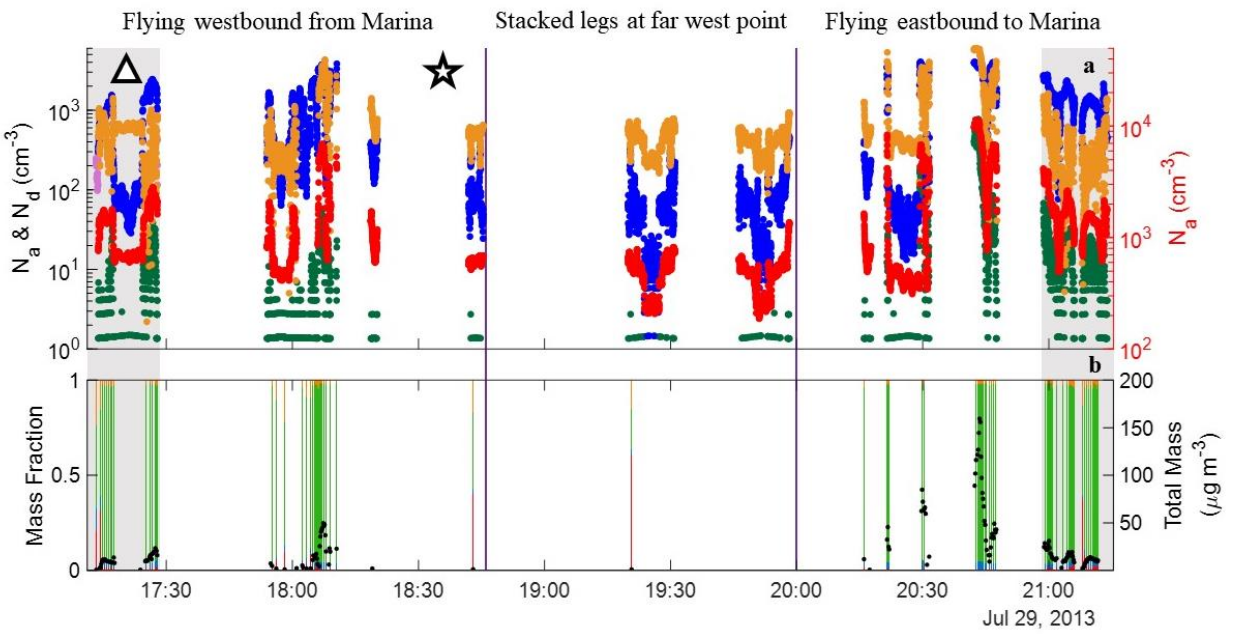

Figure S18: Data time series from NiCE RF 16 in the free troposphere (>765 m). The grey shading indicates time periods with mostly southerly winds, and the purple lines across all graphs indicate flight zones (outbound track, stacked legs at farthest west point, and inbound track; see flight map in Fig. 7a). (a) The colored points on the left-hand axis correspond to $N_{a0.1\text{-}1\mu m}$ (blue, PCASP$_{<1\mu m}$), $N_{a>1\mu m}$ (green, PCASP$_{>1\mu m}$), and N_d (light purple, CASF). The colored points on the right-hand axis correspond to $N_{a>10nm}$ (red, CPC) and $N_{a10\text{-}100nm}$ (yellow, CPC–PCASP). The triangle corresponds to the HYSPLIT back-trajectory end point seen in Fig. 5c, and the star corresponds to the HYSPLIT back-trajectory end point seen in Fig. 5b. (b) Time series of AMS mass fractions (left axis) of SO_4^{2-} (red), NO_3^- (blue), organics (green), and NH_4^+ (orange) and total mass concentration (µg m^{-3}; black points on right axis).

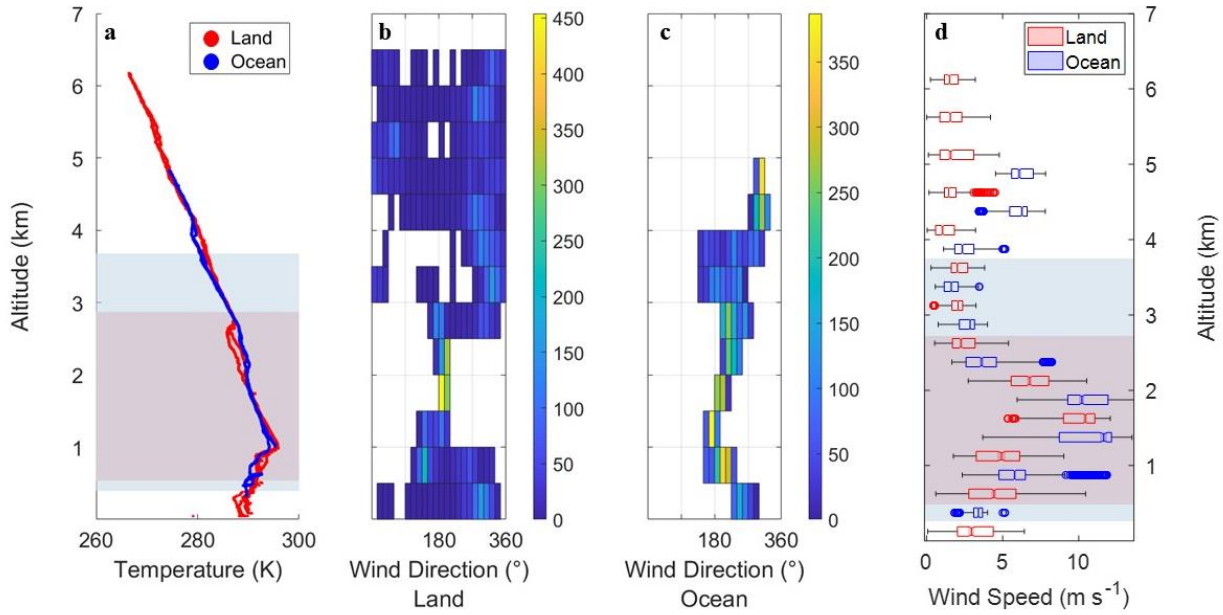

Figure S19: CSM RF 6 vertical profiles of (a) temperature, (b) wind direction over land and (c) over ocean with the color bar indicating number of points per box (500 m altitude bins and 15° wind direction bins), and (d) wind speed. The box plots show data every 500 m over land (red) and the ocean (blue) above the MBL, which is the maximum altitude of the first bins for panels b, c, and d. The shading in panels (a) and (d) indicates altitudes with southerly winds (land = red; ocean = blue).

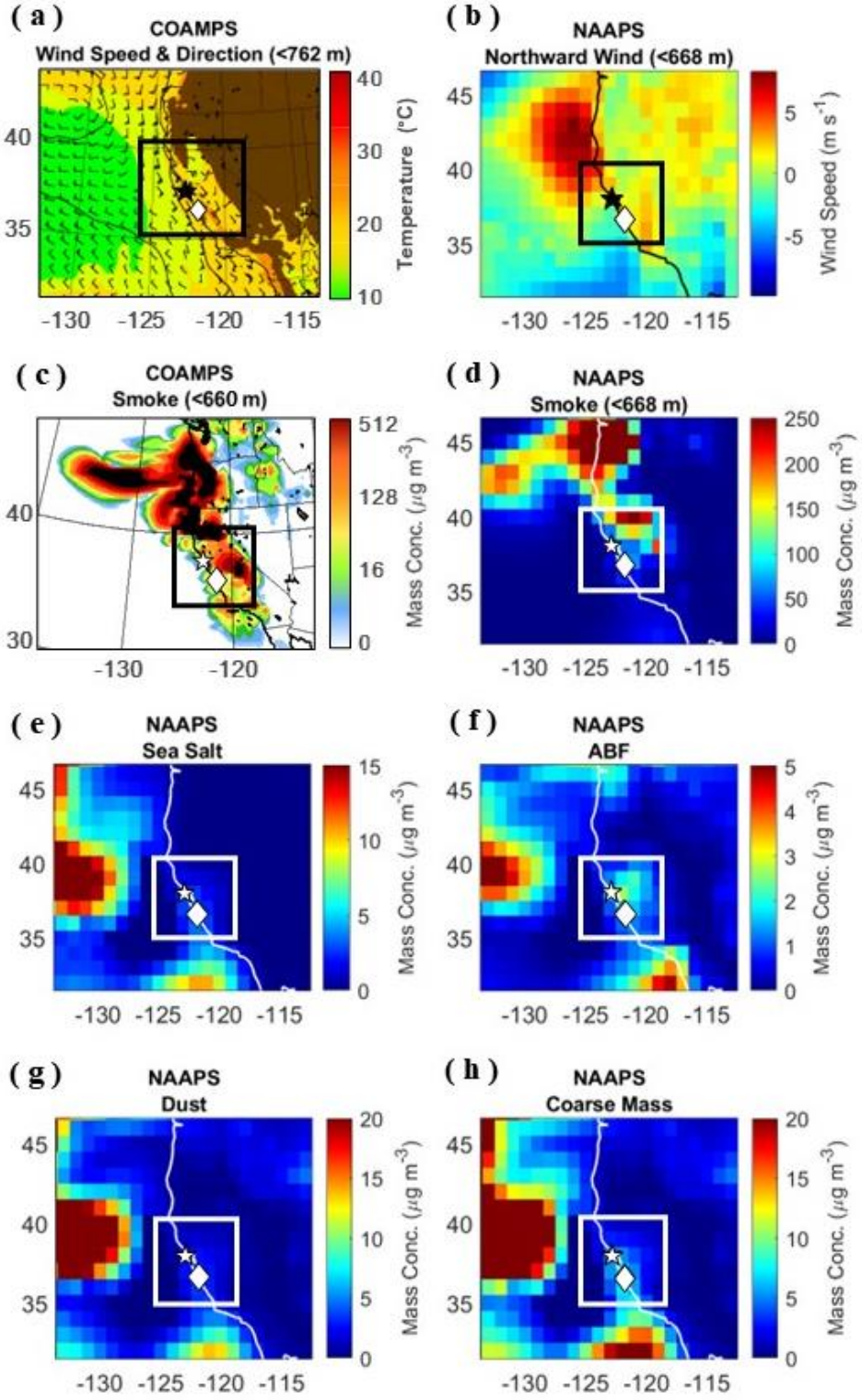

Figure S20: COAMPS/NAAPS images are for 2100 UTC. (a) Wind speed and direction up to 762 m derived from COAMPS. The colors indicate surface temperature (°C). (b) Wind speed of northward wind up to 668 m derived from NAAPS. (c) Smoke concentration (μg m^{-3}) up to 660 m derived from COAMPS. (d) Smoke, (e) sea salt, (f) ABF, (g) dust, and (h) coarse mass concentrations (μg m^{-3}) up to 668 m derived from NAAPS. The white diamond indicates Marina, CA, the white star indicates Pt. Reyes, and the black & white boxes indicate our zone of interest.